Reactivity of Mono-Meso-Substituted Iron(II) Octaethylporphyrin Complexes with Hydrogen Peroxide in the Absence of Dioxygen. Evidence for Nucleophilic Attack on the Heme

Heather Kalish,[†] Jason E. Camp,[†] Marcin Stępień,[‡] Lechosław Latos-Grażyński,[‡] and Alan L. Balch*

Contribution from the Departments of Chemistry, University of California, Davis, California 95616, and University of Wrocław, Wrocław, Poland

Received June 25, 2001

Abstract: Treatment of the mono-meso-substituted iron(II) octaethylporphyrin complexes, $(py)_2Fe^{II}$(*meso*-NO_2-OEP), $(py)_2Fe^{II}$(*meso*-CN-OEP), $(py)_2Fe^{II}$(*meso*-HC(O)-OEP), $(py)_2Fe^{II}$(*meso*-Cl-OEP), $(py)_2Fe^{II}$(*meso*-OMe-OEP), $(py)_2Fe^{II}$(*meso*-Ph-OEP), and $(py)_2Fe^{II}$(*meso*-*n*-Bu-OEP), with hydrogen peroxide in pyridine-d_5 at −30 °C in the strict absence of dioxygen has been monitored by ^{1}H NMR spectroscopy. The product oxophlorin complexes are stable as long as the samples are protected from exposure to dioxygen. Hydrogen peroxide reacts cleanly with mono-meso-substituted iron(II) porphyrins in pyridine solution under an inert atmosphere to form mixtures of three possible oxygenation products, $(py)_2Fe$(*cis-meso*-R-OEPO), $(py)_2Fe$(*trans-meso*-R-OEPO), and $(py)_2Fe$(OEPO). The yields of $(py)_2Fe$(OEPO), which results from replacemement of the unique meso substituent, as a function of the identity of the meso substituent decrease in the order NO_2 > HC(O) ∼ CN ∼ Cl > OMe > Ph, Bu, which suggests that the species responsible for attack on the porphyrin periphery is nucleophilic in nature. A mechanism involving isoporphyrin formation through attack of hydroxide ion on a cationic iron porphyrin with an oxidized porphyrin ring is suggested. The identity of the unique meso functionality also affects the regiospecificity of substitution when the unique meso group is retained. Although random attack at the two different meso sites is expected to yield a cis/trans product ratio of 2, the observed ratios vary in the following order: cyano, 5.0; *n*-butyl, 4.9; chloro, 3.2; formyl, 2.6; methoxy, 1.9; phenyl 1.4.

Introduction

Hydrogen peroxide interacts with heme proteins and hemes themselves in many significant ways. Peroxidases are heme enzymes that utilize hydrogen peroxide to generate highly oxidized hemes that are subsequently used to oxidize organic substrates,[1] while catalases are designed to destroy hydrogen peroxide through disproportionation. In both of these types of heme enzymes, the Fe(III) state reacts with hydrogen peroxide and is oxidized by two electrons to produce ferryl intermediates and heme radicals.[2,3] Although cytochrome P450 is designed to utilize dioxygen to oxidize substrates, it can also utilize hydrogen peroxide to effect the same transformations via the peroxide shunt.[4] Again, two-electron oxidation of the heme protein is involved, but reactive intermediates do not become detectable in this process. Bovine cytochrome *c* oxidase also produces an oxidized protein with a ferryl ion and a porphyrin free radical as well as a second free radical assigned as a tryptophan cation radical when it is treated with hydrogen peroxide.[5,6] Treatment of myoglobin or hemoglobin with hydrogen peroxide results in the formation of ferrylmyoglobin or ferryl hemoglobin, respectively.[7,8] Further reaction of ferryl hemoglobin is reported to result in heme degradation with the formation of fluorescent heme degradation products.[9,10] Usually, heme degradation is catalyzed by the enzyme heme oxygenase, which acts on heme as substrate and uses that heme to bind and activate dioxygen for heme cleavage.[11,12] This process requires an external electron source, and hydrogen peroxide can be employed as a substitute for dioxygen and two electrons. With hydrogen peroxide as oxidant, the heme/heme oxygenase complex is converted under anaerobic conditions[13] into the α-*meso*-hydroxyheme/heme oxygenase complex, a known intermediate in heme cleavage.[14] Electrophilic attack by an Fe^{III}−O−O−H intermediate on the heme meso position has been proposed as the mechanism for the initial step in porphyrin ring opening.[11]

The reactions of hydrogen peroxide with simple iron porphyrins, particularly with *meso*-tetra(aryl)porphyrins, have been

[†] University of California.

[‡] University of Wrocław.

(1) Everse, J.; Everse, K. E.; Grisham, M. B. *Peroxidases in Chemistry and Biology*; CRC Press: Boca Raton, FL, 1991; Vols. I and II.

(2) Weiss, R.; Gold, A.; Trautwein, A. X.; Ternier, J. In *The Porphyrin Handbook*; Kadish, K. M., Smith, K. M., Guilard, R., Eds.; Academic Press: New York, 2000; Vol. 4, p 65.

(3) Strukul, G., Ed. *Catalytic Oxidations with Hydrogen Peroxide as Oxidant*; Kluwer Academic Publishers: Boston, 1992.

(4) Ortiz de Montellano, P. R., Ed. *Cytochrome P450: Structure, Mechanism and Biochemistry*; Plenum Press: New York, 1995.

(5) Rigby, S. E. J.; Jünemann, S.; Rich, P. R.; Heathcote, P. *Biochemistry* **2000**, *39*, 5921.

(6) Fabian, M.; Palmer, G. *Biochemistry* **1995**, *34*, 13802.

(7) Balch, A. L.; La Mar, G. N.; Latos-Grayżyński, L.; Renner, M. W.; Trhanabal, V. *J. Am. Chem. Soc.* **1985**, *107*, 3003.

(8) Giulivi, C.; Davies, K. J. A. *Methods Enzymol.* **1994**, *186*, 490.

(9) Nagababu, E.; Rifkind, J. M. *Biochemistry* **2000**, *39*, 12503.

(10) Nagababu, E.; Rifkind, J. M. *Biochem. Biophys. Res. Commun.* **1998**, *247*, 592.

(11) Ortiz de Montellano, P. R.; Wilks, A. *Adv. Inorg. Chem*. **2001**, *51*, 359.

(12) Yoshida, T.; Migita, C. T. *J. Inorg. Biochem.* **2000**, *82*, 33.

(13) Liu, Y.; Moënne-Loccoz, P.; Loehr, T. M.; Ortiz de Montellano, P. R. *J. Biol. Chem*. **1997**, *272*, 6909.

(14) Balch, A. L. *Coord. Chem. Rev.* **2000**, *200*−*202*, 349.

10.1021/ja011545b CCC: $20.00
Published on Web 11/01/2001

Scheme 1

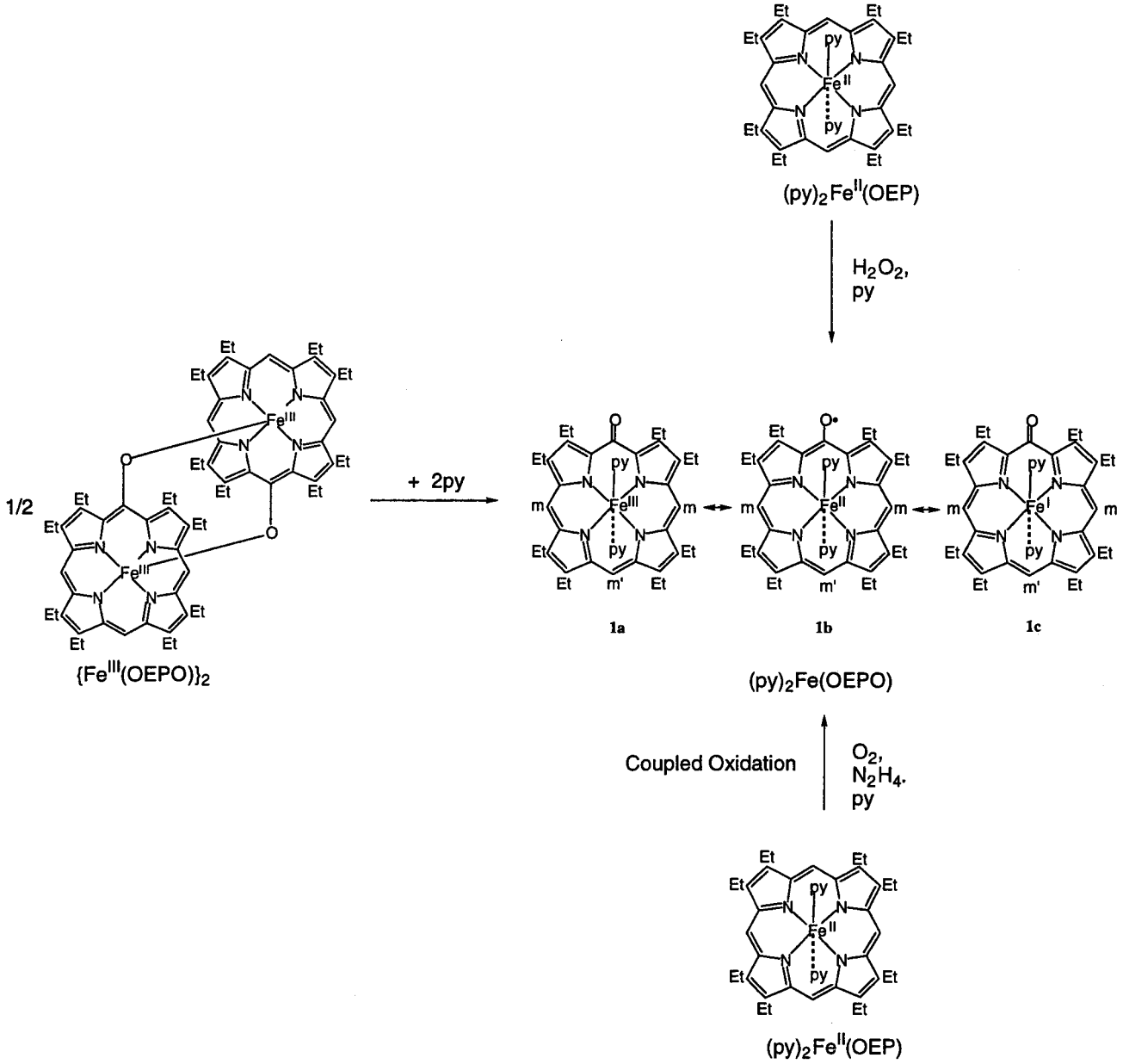

utilized to effect olefin epoxidation as well as hydrocarbon hydroxylation.[15] However, reactions of hydrogen peroxide with iron porphyrins frequently are accompanied by bleaching and catalyst destruction. Consequently, a number of porphyrins have been synthesized with substituent patterns designed to reduce their susceptibility to peripheral oxidation.[16,17] The results reported here investigate the earliest stages in the heme modification by hydrogen peroxide in cases where most of the porphyrin meso sites are not protected by the presence of aryl substituents.

Recently we have shown that treatment of $(py)_2Fe^{II}(OEP)$ with hydrogen peroxide in pyridine solution results in the formation of the *meso*-oxygenated heme $(py)_2$(FeOEPO) as shown in Scheme 1.[18] The air-sensitive $(py)_2$(FeOEPO) has been the subject of considerable study[19−22] and has been crystallized and characterized by X-ray diffraction in this laboratory.[14,23]

Spectroscopically, $(py)_2$Fe(OEPO) is readily identified on the basis of its characteristic ^{1}H NMR spectrum, which displays marked upfield shifts for the two types of meso protons and both upfield and downfield shifts for the methylene protons. Addition of pyridine to the dimer, $\{Fe^{III}(OEPO)\}_2$, in the strict absence of dioxygen is another convenient route to prepare $(py)_2$Fe(OEPO), as also shown in Scheme 1.[24,25] The electronic

(15) Meunier, B.; Robert, A.; Pratviel, G.; Bernadou, J. In *The Porphyrin Handbook*; Kadish, K. M., Smith, K. M., Guilard, R., Eds.; Academic Press: New York, 2000; Vol. 4, p 119.

(16) Traylor, P. S.; Dolphin, D.; Traylor, T. G. *J. Chem. Soc., Chem. Commun.* **1984**, 279.

(17) Dolpin, D.; Traylor, T. G.; Xie, L. Y. *Acc. Chem. Res.* **1997**, *30*, 251.

(18) Kalish, H. R.; Latos-Grayżyński, L.; Balch, A. L. *J. Am. Chem. Soc.* **2000**, *122*, 12478.

(19) Sano, S.; Sugiura, Y.; Maeda, Y.; Ogawa, S.; Morishima, I. *J. Am. Chem. Soc.* **1981**, *103*, 2888.

(20) Morishima, I.; Fujii, H.; Shiro, Y. *J. Am. Chem. Soc.* **1986**, *108*, 3858.

(21) Morishima, I.; Shiro, Y.; Hiroshi, F. *Inorg. Chem.* **1995**, *34*, 1528.

(22) Balch, A. L.; Noll, B. C.; Reid, S. M.; Zovinka, E. P. *Inorg. Chem.* **1993**, *32*, 2610.

(23) Balch, A. L.; Koerner, R.; Latos-Grayżyński, L.; Noll, B. C. *J. Am. Chem. Soc.* **1996**, *118*, 2760.

(24) Balch, A. L.; Latos-Grayżyński, L.; Noll, B. C.; Olmstead, M. M.; Zovinka, E. P. *Inorg. Chem.* **1992**, *31*, 2248.

structure of $(py)_2Fe(OEPO)$ can be described by a combination of the three canonical structures shown as **1a**, **1b**, and **1c** in Scheme 1. While the crystallographic data on this species indicate that the iron is in a high spin state,[7] the assignment of oxidation states to the iron and ligand in this complex is less clear, particularly in solution where the magnetic properties indicate that changes in the magnetic coupling between metal and ligand occur. Coupled oxidation of $(py)_2Fe^{II}(OEP)$ in pyridine solution also produces $(py)_2(FeOEPO)$ as a detectable intermediate. The coupled oxidation process, in which heme degradation is brought about by dioxygen in the presence of a reducing agent (generally hydrazine or ascorbic acid), has been widely employed as a model for biological heme catabolism.[26−28] This coupled oxidation procedure can be utilized to oxidize both iron porphyrins[29,30] and heme proteins such as myoglobin.[31,32]

Here we report on the reaction of hydrogen peroxide with simple mono-meso-substituted iron(II) octaethylporphyrins under carefully controlled conditions.

Results and Discussion

The reactions of the mono-meso-substituted iron(II) porphyrins, $(py)_2Fe^{II}$(*meso*-NO_2-OEP), $(py)_2Fe^{II}$(*meso*-HC(O)-OEP), $(py)_2Fe^{II}$(*meso*-CN-OEP), $(py)_2Fe^{II}$(*meso*-Cl-OEP), $(py)_2Fe^{II}$(*meso*-OMe-OEP), $(py)_2Fe^{II}$(*meso*-Ph-OEP), and $(py)_2Fe^{II}$(*meso*-*n*-Bu-OEP), with hydrogen peroxide were conducted at −30 °C in the absence of dioxygen. Red pyridine-d_5 solutions of these low-spin ($S = 0$) complexes were prepared under a dinitrogen atmosphere to exclude any oxidation by dioxygen and cooled to −30 °C. Introduction of dioxygen-free hydrogen peroxide (50% in water)/pyridine-d_5 solution (1/60 v/v) into the sample produced a color change to brownish green. The ^{1}H NMR spectra of the resulting solutions showed the presence of new sets of resonances due to the new, paramagnetic products. After reaction there was no evidence for the formation of any precipitate, and so the spectral data are indicative of the entire course of the reaction. Once formed at −30 °C, the resulting samples are stable and can be warmed to room temperature and above without further reaction as long as they are protected from dioxygen.

As shown in Scheme 2, the reaction of a mono-meso-substituted iron porphyrin with hydrogen peroxide can result in the formation of three products, $(py)_2Fe$(*cis-meso*-R-OEPO), $(py)_2Fe$(*trans-meso*-R-OEPO), and $(py)_2Fe$(OEPO). Air-sensitive $(py)_2Fe$(OEPO), which forms if the meso substituent itself is replaced in the reaction with hydrogen peroxide, is readily identified on the basis of its characteristic ^{1}H NMR spectrum (see trace B of Figure 1).[14,18,20,21] The ^{1}H NMR spectra of $(py)_2Fe$(*cis-meso*-R-OEPO) and $(py)_2Fe$(*trans-meso*-R-OEPO) can be readily distinguished and identified since they differ in symmetry. For example, $(py)_2Fe$(*cis-meso*-R-OEPO) will display two equally intense meso resonances (corresponding to individual protons), while $(py)_2Fe$(*trans-meso*-R-OEPO) will display only one meso proton resonance (corresponding to two meso protons). Additionally, $(py)_2Fe$(*trans-meso*-R-OEPO) will display four equally intense methylene resonances, while $(py)_2Fe$(*cis-meso*-R-OEPO) will produce eight equally intense methylene resonances.

Scheme 2

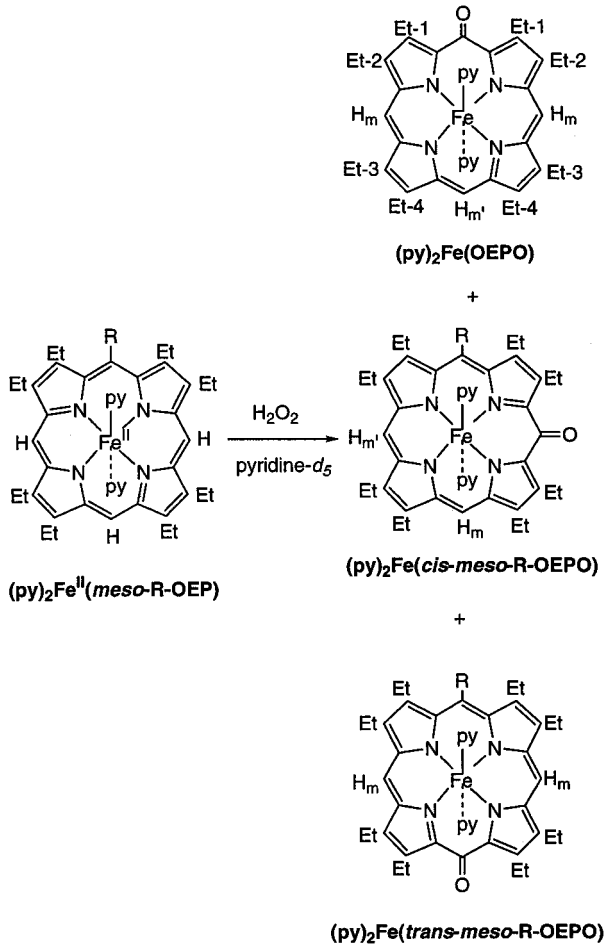

Part A of Figure 1 shows ^{1}H NMR spectra resulting from the addition of hydrogen peroxide to a pyridine-d_5 solution of $(py)_2Fe^{II}$(*meso*-Cl-OEP). Part B of this figure shows the ^{1}H NMR spectrum of $(py)_2Fe$(OEPO) which was prepared by dissolving $\{Fe^{III}(OEPO)\}_2$ in pyridine-d_5 under an inert atmosphere. The resonances in this spectrum have all been assigned on the basis of integrated resonance intensity and 1D NOE difference spectra as reported previously.[18] Three regions of the spectrum are of particular importance in analyzing the new data reported here. The far upfield region contains the meso proton resonances which are broadened because of their proximity to the paramagnetic iron ion. The downfield region at ca. 30 ppm consists of well-separated resonances due to the methylene protons in position 2 (see Scheme 2), while the methylene protons at position 1, which is closest to the oxygen atom of the tetrapyrrole, produce a resonance at −8 ppm. All the other resonances of $(py)_2Fe$(OEPO) are crowded into the region between 5 and −2 ppm and are less useful in identifying components in complex product mixtures.

Comparison of the spectra in traces A and B reveals that $(py)_2Fe$(OEPO) is a significant product of the reaction of $(py)_2Fe^{II}$(*meso*-Cl-OEP) with hydrogen peroxide. However, the presence of additional resonances indicates that $(py)_2Fe$(*cis-meso*-Cl-OEPO) and $(py)_2Fe$(*trans-meso*-Cl-OEPO) are formed as well. Thus, in the far upfield meso region there are three additional resonances. Examination of the integrated intensities of these resonances indicates that the resonances at −125 and

(25) Balch, A. L.; Noll, B. C.; Reid, S. M.; Zovinka, E. P. *Inorg. Chem.* **1993**, *32*, 2610.
(26) Warburg, O.; Negelein, E. *Chem. Ber.* **1930**, *63*, 1816.
(27) Lagarias, J. C. *Biochim. Biophys. Acta* **1982**, *717*, 12.
(28) St. Claire, T. N.; Balch, A. L. *Inorg. Chem.* **1999**, *38*, 684.
(29) Balch, A. L.; Latos-Grayżyński, L.; Noll, B. C.; Olmstead, M. M.; Szterenberg, L.; Safari, N. *J. Am. Chem. Soc.* **1993**, *115*, 1422.
(30) Balch, A. L.; Latos-Grayżyński, L.; Noll, B. C.; Olmstead, M. M.; Safari, N. *J. Am. Chem. Soc.* **1993**, *115*, 9056.
(31) O'Carra, P.; Colleran, E. *FEBS Lett.* **1969**, *5*, 295.
(32) Hildebrand, D. P.; Tang, H.; Luo, Y.; Hunter, C. L.; Smith, M.; Brayer, G. D.; Mauk, A. G. *J. Am. Chem. Soc.* **1996**, *118*, 12909.

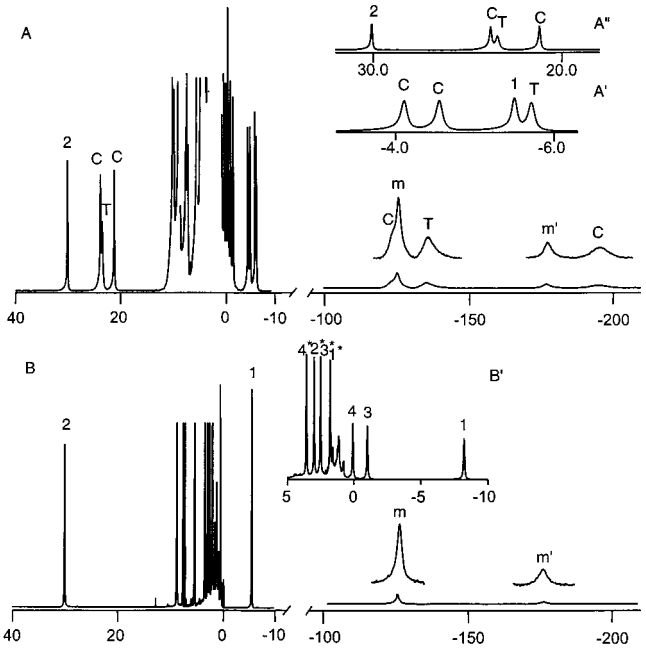

Figure 1. (A) The 500 MHz ^{1}H NMR spectrum of a pyridine-d_5 solution of $(py)_2Fe^{II}$(*meso*-Cl-OEP) after treatment with hydrogen peroxide at −30 °C and warming to 0 °C. Inset A″ shows an expansion of the downfield methylene region, while inset A′ shows the upfield methylene region. (B) The 500 MHz ^{1}H NMR spectrum of a pyridine-d_5 solution of $(py)_2Fe$(OEPO). Inset B′ shows an expansion of the spectrum from 5 to −10 ppm. Resonances of $(py)_2Fe$(OEPO) are labeled m and m′ for the meso proton resonances, 1−4 for the methylene protons corresponding to the numbering given in Scheme 1, and 1*−4* for the methyl protons as numbered in Scheme 1. Resonances of $(py)_2Fe$(*cis-meso*-Cl-OEPO) and $(py)_2Fe$(*trans-meso*-Cl-OEPO) are labeled C and T, respectively.

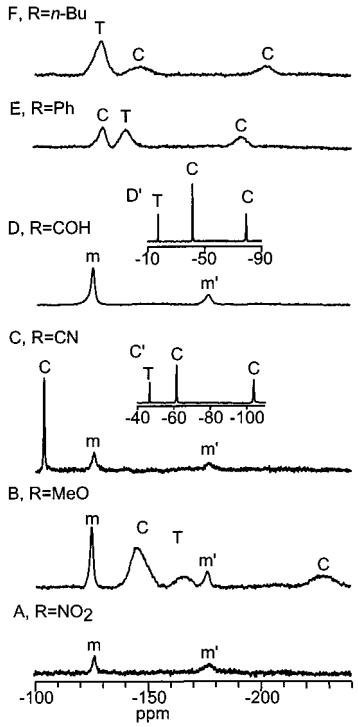

Figure 2. The far upfield meso region of the 500 MHz ^{1}H NMR spectra obtained from the reaction of hydrogen peroxide with (A) $(py)_2Fe^{II}$(*meso*-NO_2-OEP), (B) $(py)_2Fe^{II}$(*meso*-OMe-OEP), (C) $(py)_2Fe^{II}$(*meso*-CN-OEP), (D) $(py)_2Fe^{II}$(*meso*-HC(O)-OEP), (E) $(py)_2Fe^{II}$(*meso*-Ph-OEP), and (F) $(py)_2Fe^{II}$(*meso*-*n*-Bu-OEP) in pyridine-d_5. Addition of hydrogen peroxide was conducted at −30 °C, and the samples were warmed to 0 °C, where the spectra were recorded. The inset to trace C shows the −40 to −110 ppm region of the spectrum, where the resonances of the cis and trans isomers are found. The inset to trace D shows the −10 to −90 ppm region of the spectrum, where the resonances of the cis and trans isomers are found. Resonances of $(py)_2Fe$(OEPO) are labeled m and m′, while those of the cis and trans isomers are labeled C and T, respectively.

−195 ppm have equal intensity, and these resonances are assigned to $(py)_2Fe$(*cis-meso*-Cl-OEPO). The remaining resonance at −140 ppm is assigned to $(py)_2Fe$(*trans-meso*-Cl-OEPO), which is expected to produce only a single resonance from the two equivalent meso protons. Similarly, in the downfield methylene region (from 20 to 30 ppm) there are three resonances in addition to the resonance of $(py)_2Fe$(OEPO). Inset A″ of Figure 1 shows an expansion of this region. The two equally intense resonances at 22 and 23.5 ppm are assigned to the methylene groups of $(py)_2Fe$(*cis-meso*-Cl-OEPO), while the remaining resonance at 23 ppm is assigned to the methylene protons of $(py)_2Fe$(*trans-meso*-Cl-OEPO). Finally, in the 0 to −10 ppm region, which is shown in expanded form in inset A′ of Figure 1, there are also four resonances: two equally intense resonances from $(py)_2Fe$(*cis-meso*-Cl-OEPO), a unique resonance from $(py)_2Fe$(*trans-meso*-Cl-OEPO), and the clearly identifiable resonance from $(py)_2Fe$(OEPO). Careful examination of the integrated intensities of the resonances in each region reveals that the compounds $(py)_2Fe$(OEPO), $(py)_2Fe$(*cis-meso*-Cl-OEPO), and $(py)_2Fe$(*trans-meso*-Cl-OEPO) are formed in ratios of 1:2.7:1.

Similar reactions of hydrogen peroxide with other monomeso-substituted iron(II) octaethylporphyrins have been conducted. Figure 2 shows portions of the ^{1}H NMR spectra in the far upfield region that result from treating samples of $(py)_2Fe^{II}$(*meso*-NO_2-OEP) (trace A), $(py)_2Fe^{II}$(*meso*-MeO-OEP) (trace B), $(py)_2Fe^{II}$(*meso*-CN-OEP) (trace C), $(py)_2Fe^{II}$(*meso*-HC(O)-OEP) (trace D), $(py)_2Fe^{II}$(*meso*-Ph-OEP) (trace E), and $(py)_2Fe^{II}$(*meso*-*n*-Bu-OEP) (trace F) with hydrogen peroxide. As can be seen in trace A, for $(py)_2Fe^{II}$(*meso*-NO_2-OEP) the spectrum consists only of resonances due to $(py)_2Fe$(OEPO); there is no evidence for the formation of the potential products $(py)_2Fe^{II}$(*cis-meso*-NO_2-OEP) and $(py)_2Fe^{II}$(*trans-meso*-NO_2-OEP). In traces B, C, and D, there are five resonances in the upfield region, and consequently all three possible products form from these three mono-meso-substituted porphyrins. However, for $(py)_2Fe^{II}$(*meso*-Ph-OEP) and $(py)_2Fe^{II}$(*meso*-*n*-Bu-OEP), as can be seen in traces E and F, respectively, there is no evidence for the formation of $(py)_2Fe$(OEPO). However, in both cases resonances from the corresponding cis and trans isomers of the substituted oxygenated hemes are observed. The assignment of resonances in this region has been made through careful integration of the resonance intensities at several temperatures whenever there was a difficult assignment. For example, in trace B the upfield resonance labeled C is so broad that it does not appear to have the same intensity as its downfield counterpart. However, consideration of the line width together with examination of the spectrum at higher temperatures indicates that the assignment is correct.

Figure 3 shows the downfield methylene region of the ^{1}H NMR spectra of samples of $(py)_2Fe^{II}$(*meso*-MeO-OEP) (trace A), $(py)_2Fe^{II}$(*meso*-CN-OEP) (trace B), $(py)_2Fe^{II}$(*meso*-HC(O)-OEP) (trace C), $(py)_2Fe^{II}$(*meso*-Ph-OEP) (trace D), and $(py)_2Fe^{II}$(*meso*-*n*-Bu-OEP) (trace E) after treatment with hydrogen peroxide. As expected from the data shown in Figure 2, the methylene resonance of $(py)_2Fe$(OEPO) is present in traces A, B, and C but absent in traces D and E. In traces B, C, and D,

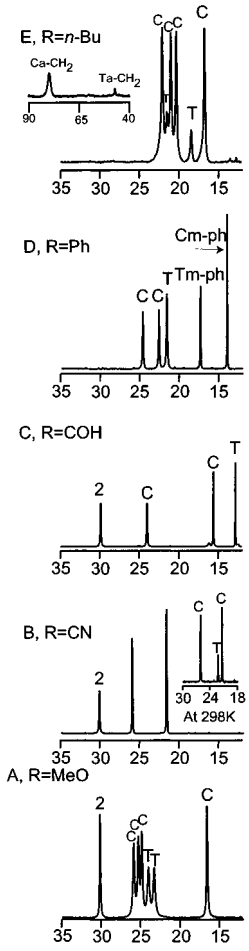

Figure 3. The downfield methylene region of the 500 MHz ^{1}H NMR spectra obtained from the reaction of hydrogen peroxide with (A) $(py)_2Fe^{II}$(*meso*-OMe-OEP), (B) $(py)_2Fe^{II}$(*meso*-CN-OEP), (C) $(py)_2Fe^{II}$(*meso*-HC(O)-OEP), (D) $(py)_2Fe^{II}$(*meso*-Ph-OEP), and (E) $(py)_2Fe^{II}$(*meso*-*n*-Bu-OEP) in pyridine-d_5. Addition of hydrogen peroxide was conducted at −30 °C, and the samples were warmed to 0 °C, where the spectra were recorded. The inset to trace B shows the spectrum at 25 °C, where the resonances of the cis and trans isomers are fully resolved. The inset to trace E shows the α-methylene resonance of the *n*-Bu group. Resonances of $(py)_2Fe$(OEPO) are labeled 2, while those of the cis and trans isomers are labeled C and T, respectively.

three other resonances appear in this window. These three resonances result from the presence of the cis and trans isomers: $(py)_2Fe$(*cis-meso*-CN-OEPO) and $(py)_2Fe$(*trans-meso*-CN-OEPO); $(py)_2Fe$(*cis-meso*-HC(O)-OEPO) and $(py)_2Fe$(*trans-meso*-HC(O)-OEPO); and $(py)_2Fe$(*cis-meso*-Ph-OEPO) and $(py)_2Fe$(*trans-meso*-Ph-OEPO).

The spectrum obtained from oxidation of $(py)_2Fe^{II}$(*meso*-MeO−OEP) with hydrogen peroxide shown in trace A of Figure 3 consists of six resonances, not the expected three, along with the resonance from $(py)_2Fe$(OEPO). The two equally intense resonances at ca. 24 ppm are assigned to the presence of $(py)_2Fe$(*trans-meso*-MeO-OEPO), while the other four resonances are assigned to $(py)_2Fe$(*cis-meso*-MeO-OEPO). Although the peak heights are unequal for these four resonances, careful integration of these resonances indicates that the four lines do have equal intensity. The doubling of the number of resonances for each of these two isomers results from restricted rotation of the *meso*-MeO group about the O−C(meso) bond. Crowding of the methoxy group between the adjacent pyrrole ethylene groups forces this group to an out-of plane location that renders the two sides of the porphyrin plane inequivalent. Similar effects

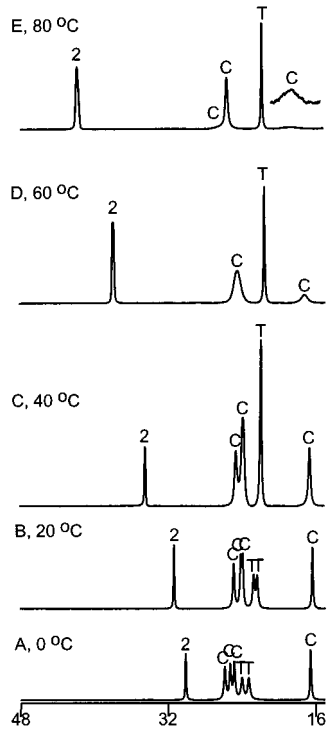

Figure 4. Temperature-dependent 500 MHz ^{1}H NMR spectra of a sample of $(py)_2Fe^{II}$(*meso*-OMe-OEP) in pyridine-d_5 after treatment with hydrogen peroxide. Resonances are labeled in accord with those used in Figure 3.

of local crowding on functional group mobility have been seen in other octaethylporphyrins with unique meso substituents.[33]

Traces D and E of Figure 3 also reveal additional resonances due to the unique meso substituents. In trace D for $(py)_2Fe$(*meso*-Ph-OEPO), two resonances at 14 and 17 ppm are assigned to the *meta* protons of the phenyl substituents of the cis and trans isomers, respectively. The relative intensities of these resonances is the same as the relative amounts of the cis and trans isomers given by the resonances in the 20−30 ppm region. The inset to trace E for $(py)_2Fe$(*meso*-Bu-OEPO) shows the downfield region where the resonances of the α-methylene protons of the *n*-butyl group are found. In this case the assignment is based on the assumption that the α-methylene protons will experience the greatest hyperfine shift for any of the *n*-butyl protons as a result of the large spin density at the meso position. Since the resonances shown in this inset are the only resonances found outside the 0−10 ppm region that are otherwise unassigned, they have been assigned to the α-methylene protons of the *n*-butyl substituent. The other resonances of the *n*-butyl group have not been detected and probably are found in the crowded region from 0 to 10 ppm. Likewise, for $(py)_2Fe$(*meso*-MeO-OEPO) we have not located the methoxy methyl resonance, which is also probably located in the crowded 0−10 ppm region.

Figure 4 shows the effects of variation in the temperature on the spectrum of the sample obtained by hydrogen peroxide oxidation of $(py)_2Fe^{II}$(*meso*-MeO-OEP). At 0 °C the four resonances of $(py)_2Fe$(*cis-meso*-MeO-OEPO) and the two resonances of $(py)_2Fe$(*trans-meso*-MeO-OEPO) are clearly distinguished. Upon warming of the sample to 40 °C, the two methylene resonances of $(py)_2Fe$(*trans-meso*-MeO-OEPO) coalesce. The four methylene resonances of $(py)_2Fe$(*cis-meso*-MeO-OEPO) also broaden and partially coalesce as the sample is

(33) Balch, A. L.; Latos-Grayżyński, L.; Noll, B. C.; Olmstead, M. M.; Zovinka, E. P. *Inorg. Chem.* **1992**, *31*, 2248.

Table 1. Percent Product Yields

	$(py)_2Fe$-(OEPO)	$(py)_2Fe$-(*cis-meso*-R-OEPO)	$(py)_2Fe$-(*trans-meso*-R-OEPO)
$(py)_2Fe^{II}$(*meso*-NO_2-OEP)	100	0	0
$(py)_2Fe^{II}$(*meso*-HC(O)-OEP)	28	54	17
$(py)_2Fe^{II}$(*meso*-CN-OEP)	22	65	13
$(py)_2Fe^{II}$(*meso*-Cl-OEP)	21.5	57	21.5
$(py)_2Fe^{II}$(*meso*-MeO-OEP)	12	57	31
$(py)_2Fe^{II}$(*meso*-Ph-OEP)	0	59	41
$(py)_2Fe^{II}$(*meso-n*-Bu-OEP)	0	83	17

warmed. Upon cooling, these changes are reversed. The changes are consistent with a dynamic process in which rotation of the methoxy group about the O−C(meso) bond renders the two sides of the porphyrin plane spectroscopically equivalent. As a result, the dynamic process causes diasteriotopic methylene protons of ethyl groups to become equivalent in a pairwise fashion. Upon warming of the sample, the methylene resonance of $(py)_2Fe$(OEPO) undergoes a marked downfield shift. This anti-Curie behavior has been observed before[20,21] and is consistent with the presence of magnetically coupled spins on the ligand and metal. The resonances of $(py)_2Fe$(*cis-meso*-MeO-OEPO) and $(py)_2Fe$(*trans-meso*-MeO-OEPO) also undergo non-Curie shifts that are less pronounced over this temperature range, in addition to the changes that result from rotation about the O−C(meso) bond.

The downfield methylene portion of the ^{1}H NMR spectrum resulting from addition of hydrogen peroxide to $(py)_2Fe^{II}$(*meso-n*-Bu-OEP) seen in trace E of Figure 3 also shows four equally intense resonances that result from $(py)_2Fe^{II}$(*cis-meso-n*-Bu-OEP), and two equally intense resonances due to $(py)_2Fe^{II}$(*trans-meso-n*-Bu-OEP). The additional resonances arise from restricted rotation of the *n*-Bu group about the C−C(meso) bond, as seen for $(py)_2Fe$(*cis-meso*-MeO-OEPO) and $(py)_2Fe$(*trans-meso*-MeO-OEPO). Increasing the sample temperature results in broadening and coalescence of these resonances in a fashion which is similar to the behavior seen in Figure 4.

Integration of the relative intensities of the various resonances in the spectra reported here allows the yields of the individual products to be calculated. The relevant data are presented in Table 1. The results given in this table have been replicated three times for each different porphyrin.

The reactivity of iron porphyrins with hydrogen peroxide is oxidation state dependent. The reactivity of iron(III) porphyrins with hydrogen peroxide has also been explored under similar conditions. Treatment of $ClFe^{III}$(OEP) or $ClFe^{III}$(*meso*-NO_2-OEP) with hydrogen peroxide in pyridine-d_5 solution does not produce a detectable change in the ^{1}H NMR spectrum of either complex. Additionally, ^{1}H NMR studies reveal that addition of potassium hydroxide to a pyridine solution of $ClFe^{III}$(OEP) or $ClFe^{III}$(*meso*-NO_2-OEP) does not form $(py)_2Fe$(OEPO) but produces new species with ^{1}H NMR spectra that are indicative of high-spin species which are presumed to be $HOFe^{III}$(OEP) or $HOFe^{III}$(*meso*-NO_2-OEP). As noted earlier in our study of the reaction of $(py)_2Fe^{II}$(OEP) with hydrogen peroxide,[18] there is no evidence for the formation of ferryl, $(Fe{=}O)^{2+}$, intermediates in the reactions of hydrogen peroxide with $(py)_2Fe^{II}$(*meso*-R-OEP).

Conclusions

Mechanism of Reaction. The results described above demonstrate that hydrogen peroxide reacts cleanly with monomeso-substituted iron(II) porphyrins in pyridine solution under an inert atmosphere to form mixtures of three possible oxygenation products, as shown in Scheme 2. These complexes are stable in pyridine solution as long as the solutions are protected from reaction with dioxygen, which transforms the oxygenated hemes into substituted biliverdins and verdohemes, as described previously for $(py)_2Fe$(OEPO).[28]

As can be seen in Table 1, the product ratios obtained in the heme/hydrogen peroxide reactions strongly depend of the identities of the meso substituents. Thus, with a nitro group at one of the meso positions, the reaction with hydrogen peroxide results in the complete removal of the nitro group. However, with a phenyl or *n*-butyl group at a meso position, there is no loss of the unique substituent, and reactivity occurs exclusively at the cis and trans meso C−H groups. Thus, the yields of $(py)_2Fe$(OEPO) as a function of the identity of the meso substituent decrease in the order NO_2 > HC(O) ∼ CN ∼ Cl > OMe > Ph, Bu. A similar trend is seen in the Swain *F* parameter (derived from Hammett σ values): NO_2 (1.00) > CN (0.90) > Cl (0.72) > OMe (0.54) > Ph (0.25) > Me (0.01).[34] These data suggest that the species responsible for attack on the porphyrin periphery is nucleophilic in nature.

Scheme 3 sets out a proposed mechanism for the transformation of $(py)_2Fe$(*meso*-R-OEP) into $(py)_2Fe$(OEPO). Conversion of $(py)_2Fe$(*meso*-R-OEP) eventually into intermediate **B** involves a two-electron oxidation, and there is ample precedent for hydrogen peroxide producing a two-electron oxidation of a heme. This process may be accomplished initially by Fenton type oxidation[35] to produce intermediate **A,** hydroxide ion, and hydroxyl radical. The latter subsequently serves as the oxidant to convert intermediate **A** into intermediate **B**. Hydroxyl radical is known to be a powerful one-electron oxidant.[36] Intermediate **B** may exist as the Fe(IV) complex as shown in the chart, or it may exist as the equivalent Fe(III)/porphyrin radical complex. Examples of both forms are known, e.g., Fe(IV), $(MeO)_2Fe^{IV}$(*meso*-tetra(mesityl)porphrin),[37] and Fe(III)/porphyrin radical, $(O_3ClO)_2Fe^{III}(OEP^{\bullet})$.[38]

The transformation of intermediate **B** into intermediate **C** is accomplished by nucleophilic attack of hydroxide ion on the heme. This reaction produces the isoporphyrin-containing intermediate **C**. There is ample precedent for nucleophilic additions to cationic metalloporphyrins[39] (particularly iron(III) tetraphenylporphyrin cation radicals)[40−42] or for nucleophilic additions to porphyrin radicals.[43−45] The addition of hydroxide ion to a cationic gold(III) tetraphenylporphyrin to produce a stable isoporphyrin complex analogous to intermediate **C** has particular significance in this regard.[46] However, as noted above,

(34) Swain, C. G.; Unger, S. H.; Rosenquist, N. R.; Swain, M. S. *J. Am. Chem. Soc*. **1983**, *105*, 492.
(35) Walling, C. *Acc. Chem. Res*. **1975**, *8*, 125.
(36) Kochi, J. A. In *Free Radicals*; Kochi, J. K., Ed.; John Wiley and Sons: New York, NY, 1973; p 673.
(37) Groves, J. T.; Quinn, R.; McMurry, J. T.; Nakamura, M.; Lang, G.; Boso, B. *J. Am. Chem. Soc*. **1985**, *107*, 354.
(38) Scheidt, W. R.; Song, H.; Haller, K. J.; Safo, M. K.; Orosz, R. D.; Reed, C. A.; Debrunner, P. G.; Schultz, C. E. *Inorg. Chem*. **1992**, *31*, 941.
(39) Vicente, M. G. H. In *The Porphyrin Handbook*; Kadish, K. M., Smith, K. M., Guillard, R., Eds.; Academic Press: San Diego, 2000; p 149.
(40) Maek, A.; Latos-Grażyński, L.; Bartczak, T. J.; Zadlo, A. *Inorg. Chem*. **1991**, *30*, 3222.
(41) Chmielewski, P.; Latos-Grażyński, L.; Rachlewicz, K. *Magn. Reson. Chem*. **1993**, *31*, S47.
(42) Rachlewicz, K.; Latos-Grażyński, L. *Inorg. Chem*. **1995**, *34*, 718.
(43) Smith, K. M.; Barnett, G. H.; Evans, B.; Martynenko, Z. *J. Am. Chem. Soc*. **1979**, *101*, 5953.
(44) Dolphin, D.; Halko, D. J.; Johnson, E. C.; Rousseau, K. In *Porphyrin Chemistry Advances*; Longo, F. R., Ed.; Ann Arbor Science Publisher, Inc.: Ann Arbor, MI, 1979; p 119.
(45) Shine, H. J.; Padilla, A. G.; Wu, S. M. *J. Org. Chem*. **1979**, *23*, 4069.

Scheme 3

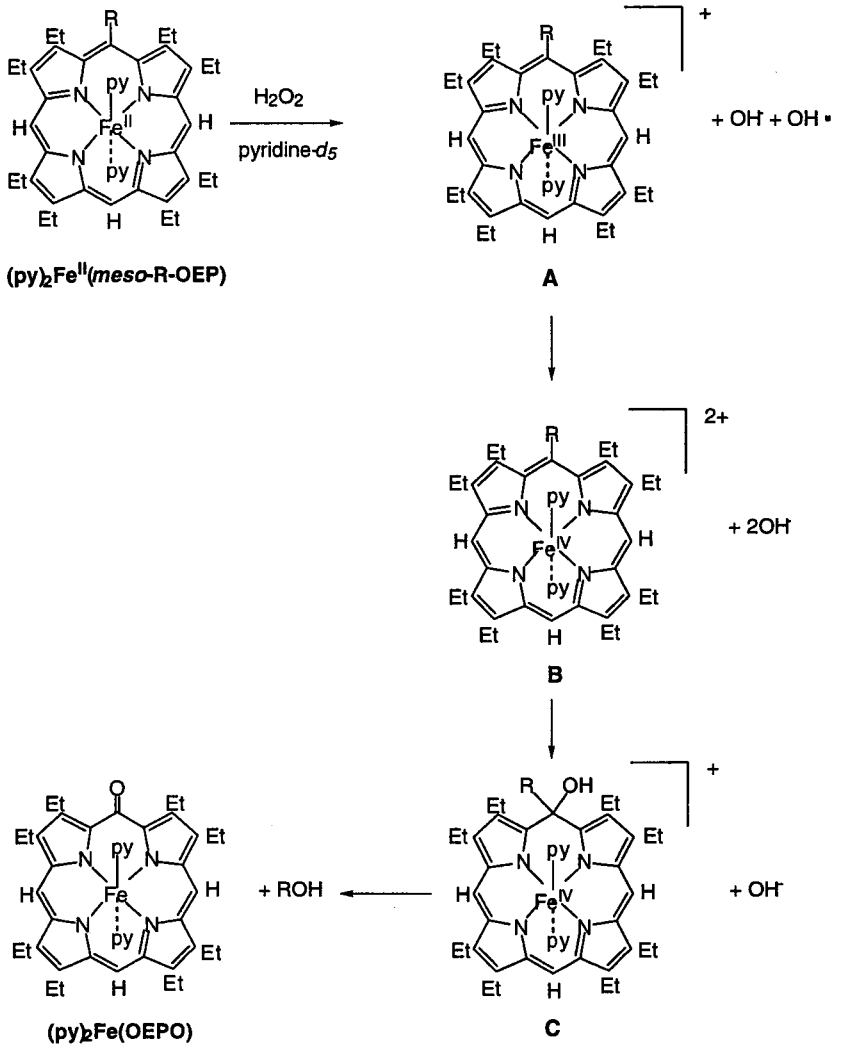

hydroxide ion does not transform iron(III) porphyrins into $(py)_2Fe(OEPO)$. Hence, we propose that the more highly oxidized intermediate **B** rather than **A** is attacked by hydroxide ion. Isoporphyrins readily revert into porphyrins through the loss of one of the substituents on the modified meso carbon.[47] Thus, the transformation from **C** into the observed product, $(py)_2Fe(OEPO)$, also has precedent. Pyridine reacts with *meso*-tetraphenylporphyrin iron(III) radical cations at the β-pyrrole sites to form stable substitution products and at the meso carbon atoms to produce less stable isoporphyrins and porphodimethenes.[48] Since there are ethyl groups in the β-pyrrole sites in the porphyrins studied here, these sites are protected from attack by hydroxide or pyridine, and initial addition is directed to the unprotected meso sites. However, pyridine is known to add to the π-cation radicals of magnesium(II) porphyrins to yield *meso*-pyridinium porphyrin salts.[49,50] In the mechanism proposed in Scheme 3, pyridine may add reversibly to the meso sites of intermediate **B**, but the overall reaction may be driven to the observed products by the addition of hydroxide, which becomes irreversible through loss of a proton on the hydroxyl group.

The identity of the unique meso functionality also affects the regiospecificity of substitution in those cases where that unique meso group is retained. Thus, while random attack at the two different meso sites is expected to yield a cis/trans product ratio of 2, the observed ratios vary in the following order: cyano, 5.0; *n*-butyl, 4.9; chloro, 3.2; formyl, 2.6; methoxy, 1.9; phenyl 1.4. Thus, the iron porphyrins with cyano and *n*-butyl substituents, with their very different electron-withdrawing and -donating characteristics, produce the greatest preference for cis substitution. Several factors may be involved in causing these variations in attack at the two different meso positions. The introduction of a unique meso substituent will alter the nature of the porphyrin π-orbitals. The modified versions of the frontier $3a_{2u}$-like and the 4e-like orbitals, which have large amplitudes at the porphyrin meso positions, provide means of electronic communication between these seemingly remote meso sites. Even steric factors may be involved. The environment of the meso sites in hemes has been recognized to be sterically constricted.[51] Introduction of a unique meso substituent will limit the conformational flexibility of the adjacent ethyl substituents in these modified porphyrins, and these constraints can be felt throughout the macrocycle. For example, the unique meso substituent in high-spin, five-coordinate ClFe(*meso*-R-OEP) Fe(III) has been found to warp the porphyrin surface away from the symmetrical dome shape found for $ClFe^{III}(OEP)$.[52] In the cases studied so far, each substituent causes a distinctively

(46) Segawa, H.; Azumi, R.; Shimadzu, T. *J. Am. Chem. Soc*. **1992**, *114*, 7564.

(47) Dolphin, D.; Felton, R. H.; Borg, D. C.; Fajer, J. *J. Am. Chem. Soc*. **1970**, *73*, 1970.

(48) Rachlewicz, K.; Latos-Grayżyński, L. *Inorg. Chem.* **1996**, *35*, 1136.

(49) Barnett, G. H.; Evans, B.; Smith, K. M.; Besecke, S.; Fuhrhop, J.-H. *Tetrahedron Lett.* **1976**, 4009.

(50) Fuhrhop, H.-J.; Wanja, U.; Bunzel, M. *Liebigs Ann. Chem*. **1984**, 426.

(51) Woodward, R. B. *Angew. Chem.* **1960**, *72*, 651.

different change in the structure. Consequently, it is not possible at this stage to make predictions about the nature of the distortion caused by these new meso substituents to either the electronic or the geometric structures of the modified porphyrin macrocycles.

The observations described here for the reaction of mono-meso-substituted iron(II) porphyrins with hydrogen peroxide contrast with the behavior observed for heme oxygenase. In that reaction, the mechanism proposed for the initial phase of heme degradation is postulated to involve electrophilic attack by an $Fe^{III}-O-O-H$ species on a meso carbon of the heme.[11] It is probable that the difference in these two reactions results from independent means of attack on the heme. In the present work with the strongly ligating environment provided by pyridine solution, the formation of an $Fe^{III}-O-O-H$ species is inhibited. However, the mechanism set out in Scheme 3 provides an alternate means of accomplishing the same result, heme oxygenation.

Mono-meso-substituted iron(II) porphyrins have also been used as substrates for heme oxygenase. Their behavior in this reaction contrasts with the observations made here for the reactions with hydrogen peroxide. Remarkably, α-*meso*-methyl-protoheme reacts with dioxygen and heme oxygenase to yield α-biliverdin.[53,54] The α-methyl substituent does not protect the attached meso carbon atom from oxidation as the butyl group does in the reactions studied in this paper. However, the fate of the meso carbon and its attached methyl group is not known. In contrast, the reaction of *meso*-formyl-substituted hemes with heme oxygenase yields biliverdins that retain appended formyl groups.[55] Thus, α-*meso*-formyl-mesoheme does not yield α-biliverdin when treated with heme oxygenase. The presence of a formyl group inhibits oxidation at the adjacent meso site. In contrast, in the reaction of $(py)_2Fe^{II}$(*meso*-HC(O)-OEP) with hydrogen peroxide, as shown in Table 1, there is considerable loss of the formyl substituent and the formation of $(py)_2$Fe-(OEPO).

The coupled oxidation of iron porphyrins in pyridine has long been used as a model for heme oxidase.[56] In this environment, oxidation of protoheme by coupled oxidation gives a mixture of the four possible isomeric biliverdins.[57] However, the results described here suggest that reactions in pyridine, which presents a strongly ligating environment, can occur through an independent mechanism as presented in Scheme 3 for the reaction with hydrogen peroxide. At this point there is no model that allows the oxidation of heme to be probed in a less strongly ligating environment that might more effectively model the protein environment in heme oxygenase to examine the intrinsic specificity of heme attack.

Electronic Structure of the Oxygenated Intermediates. The patterns of hyperfine shifts for the newly formed intermediates, $(py)_2$Fe(*cis-meso*-R-OEPO) and $(py)_2$Fe(*trans-meso*-OEPO), resemble that of $(py)_2$Fe(OEPO), itself. Thus, all compounds show meso resonances with upfield shifts, methylene resonances with both upfield and downfield shifts, and methyl resonances in the 5−0 ppm region. The meso proton resonances show the greatest variation in shifts. The single meso resonance is found at −17 ppm for $(py)_2$Fe(*trans-meso*-HC(O)-OEPO) at 0 °C, while the corresponding resonance occurs at −168 ppm for $(py)_2$Fe(*trans-meso*-MeO-OEPO) (again at 0 °C). Since all new intermediates observed in this work display spectral patterns similar to that of $(py)_2$Fe(OEPO), all involve the set of electronic distributions seen in Scheme 1, with the meso substituent offering a perturbation on the varying contributions of each resonance form: **A**, **B**, and **C**. The hyperfine shift of the meso proton resonances is dominated by the location of the individual proton relative to the oxygen atom on the porphyrin periphery. Consideration of the spectrum of $(py)_2$Fe(OEPO) suggests that the protons trans to the oxygen atom (those labeled $H_{m'}$ in Scheme 3) are expected to have chemical shifts that are upfield of the resonances from the protons (H_m) that are cis to the oxygen atom. Thus, for each cis isomer the downfield meso resonance is assigned to H_m, and the upfield resonance is assigned to $H_{m'}$. Inspection of the data in Figure 3 and the chemical shifts for the meso resonances of these intermediates in Table 2 reveals that the chemical shift for the meso proton of the trans isomer is similar to that of one of the meso protons of the cis isomer and far downfield from the other meso proton resonance of the cis isomer. This is consistent with the fact that the trans isomer possesses only meso protons (H_m) which are cis to the oxygen atom. Finally, as can be seen in Table 2, the meso proton resonances generally show a shift downfield as the electron-withdrawing nature of the unique meso substituent increases. However, $(py)_2$Fe(*trans-meso*-MeO-OEPO) does not follow this trend. The electron-withdrawing substituents in $(py)_2$Fe(*trans-meso*-NC-OEPO) and $(py)_2$Fe(*trans-meso*-HC(O)-OEPO) produce marked downfield shifts of the meso proton resonances.

Table 2. Chemical Shifts (in ppm) for Meso Proton Resonances at 0 °C

	cis isomer H_m	*cis* isomer $H_{m'}$	*trans* isomer H_m
$(py)_2$Fe(*meso*-OMe-OEPO)	−152	−226	−168
$(py)_2$Fe(*meso*-*n*-Bu-OEPO)	−146	−202	−129
$(py)_2$Fe(*meso*-Ph-OEPO)	−130	−191	−140
$(py)_2$Fe(OEPO)	−127[a]	−178[b]	
$(py)_2$Fe(*meso*-Cl-OEPO)	−125	−195	−140
$(py)_2$Fe(*meso*-CN-OEPO)	−61	−104	−47
$(py)_2$Fe(*meso*-HC(O)-OEPO)	−41	−79	−17

[a] Since there are no isomers, this is the H_m resonance. [b] Since there are no isomers, this is the $H_{m'}$ resonance

Additionally, the ^{1}H NMR spectra of $(py)_2$Fe(*cis-meso*-R-OEPO) and $(py)_2$Fe(*trans-meso*-R-OEPO) show non-Curie behavior under variable temperature conditions. For example, in addition to the effects of molecular rotation seen in Figure 4, the methylene resonances of all three species present show decidedly non-Curie shifts upon warming. This non-Curie behavior must result from variation in the coupling interactions between the metal- and ligand-based spins in these intermediates as previously discussed for $(py)_2$Fe(OEPO).[14,18,20,21,23]

Experimental Section

Materials. Octaethylporphyrin and iron(III) octaethylporphyrin chloride were purchased from Mid Century. Hydrogen peroxide, 50 wt % in water, was purchased from Aldrich. The mono-meso-substituted porphyrins, *meso*-NO_2-H_2OEP,[58] *meso*-CN-H_2OEP,[59] *meso*-Cl-H_2OEP,[60]

(52) Kalish, H.; Camp, J. E.; Stepień, M.; Latos-Grayżyński, L.; Olmstead, M. M.; Balch, A. L., manuscript in preparation.
(53) Torpey, J.; Ortiz de Montellano, P. R. *J. Biol. Chem.* **1996**, *271*, 26067.
(54) Torpey, J.; Lee, D. A.; Smith, K. M.; Ortiz de Montellano, P. R. *J. Am. Chem. Soc.* **1996**, *118*, 9172.
(55) Torpey, J.; Ortiz de Montellano, P. R. *J. Biol. Chem.* **1997**, *272*, 22008.
(56) Warburg, O.; Negelein, E. *Chem. Ber.* **1930**, *63*, 1816.
(57) Bonnett, R.; McDonagh, A. F. *J. Chem. Soc., Perkin Trans. 1* **1973**, 881.
(58) Bonnett, R.; Stephenson, G. F. *J. Org. Chem.* **1965**, *30*, 2791.
(59) Johnson, A. W.; Oldfield, D. *J. Chem. Soc. (C)* **1966**, 794.
(60) Bonnett, R.; Gale, A. D.; Stephenson, G. F. *J. Chem. Soc. (C)* **1966**, 1600.

meso-MeO-H_2OEP,[61] *meso*-Ph-H_2OEP,[62] *meso*-*n*-Bu-H_2OEP,[60] and *meso*-*n*-HC(O)-H_2OEP,[63] were prepared as described previously. Iron was inserted by a standard procedure to yield the five-coordinate chloro complexes, $ClFe^{III}$(*meso*-R-OEP).[64] The bis(pyridine)iron(II) porphyrins were subsequently prepared by reduction of the appropriate iron(III) complex with zinc amalgam in pyridine solution in a controlled atmosphere drybox under purified dinitrogen. Although generally this reduction went smoothly to produce the corresponding iron(II) porphyrin, the reduction of $ClFe^{III}$(*meso*-HC(O)-OEP) must be stopped after 5 min and the sample separated from the reducing agent. Longer reaction times result in further reactions to produce $(py)_2Fe^{III}$(*meso*-$HOCH_2$-OEP) and other unidentified products.[65]

Reactions with H_2O_2. In a controlled nitrogen atmosphere box, a dioxygen-free pyridine-d_5 solution of the bis(pyridine)iron(II) porphyrin (3−4 mmol) was placed in an NMR tube and sealed with a rubber septum and Parafilm. This solution was cooled to −30 °C in an ethanol/liquid nitrogen bath. Dioxygen was removed from hydrogen peroxide samples by five freeze/pump/thaw cycles. A pyridine-d_5 solution of hydrogen peroxide (60:1) was added via microsyringe to the porphyrin solution at −30 °C to give hydrogen peroxide concentrations in the range of 4−6 mmol. The progress of the reaction was followed by ^{1}H NMR spectroscopy.

Instrumentation. ^{1}H NMR spectra were recorded on a Bruker Avance 500 FT spectrometer (^{1}H frequency is 500.13 MHz). The spectra were recorded over a 100-kHz bandwidth with 64K data points and a 5-μs 90° pulse. For a typical spectrum, between 500 and 1000 transients were accumulated with a 50-ms delay time. The residual ^{1}H resonances in the solvent, pyridine- d_5, were used as a secondary reference.

Acknowledgment. We thank the NIH (Grant GM-26226, A.L.B.) and the Foundation for Polish Science (L.L.G.) for financial support and the NSF (Grant OSTI 97-24412) for partial funding of the 500 MHz NMR spectrometer.

JA011545B

(61) Barnett, G. H.; Hudson, M. F.; McCombie, S. W.; Smith, K. M. *J. Chem. Soc. Perkin Trans. 1* **1973**, 691.

(62) Kalisch, W. W.; Senge, M. O. *Angew. Chem., Int. Ed.* **1998**, *37*, 1107.

(63) Inhoffen, H. H.; Fuhrop, J.-H.; Voit, H.; Brockman, H. *Ann. Chem.* **1966**, *695*, 133.

(64) Adler, A. D.; Longo, F. R.; Kampas, F. *J. Inorg. Nucl. Chem.* **1970**, *32*, 2443.

(65) Kalish, H. R. Ph.D. Thesis, Univeristy of California, Davis, 2001.